Research on cloud removal based on fusing Multi-temporal Remote Sensing Images

Xuechao Zou[1], Yi Zhao[1], Pin Tao[2], and Yachao Cui[1]

[1]Qinghai University, Department of Computer Technology and Applications, Xining, China, 810016
[2]Tsinghua University, Department of Computer Technology and Applications, Beijing, China, 100084

Key Points:

- remote sensing
- cloud removal
- multi temporal
- image fusion

Corresponding author: Yachao Cui, yachaocui@163.com

Abstract

Cloud and cloud shadow are the primary factors that affect the application of remote sensing images, and they have always been problems encountered in remote sensing image processing. This article puts forward a new cloud removal strategy, whose data is from the Landsat multi-source remote sensing images and based on an improved BP neural network. Compared with the previous cloud removal methods, the selection value of BP neural network training is changed to reduce human participation. The previous gray-scale value group marked by classification (Vegetation, water body, bare land, residential land, and fields, etc.) is changed to the gray-scale value group of the two images' common areas without cloud. The experimental results show that the de-cloud image got by our method has higher SSIM and Cosine similarity with the reference image.

1 Introduction

With the wide application of Google Earth in daily life, remote sensing images have become a part of people's life (Lin et al., 2013). Therefore, remote sensing data processing has become the focus of current research. In particular, clouds and cloud shadows have become the main noise in satellite remote sensing data (Guo, 2017). At any time, an average of 35% of the world's land surface area will be covered by clouds (Wei et al., 2015). From 2013 to 2017, in the remote sensing images of 966708 Landsat 8 scenes, the overall average cloud cover of the land was as high as 41.59% (Shi, 2018). Therefore, the research on the cloud removal strategy of remote sensing images is becoming more and more important.

To solve the problem of cloud removal of remote sensing images, researchers have proposed a lot of cloud removal algorithms. According to the thickness of clouds, the methods of removing clouds can be divided into two categories: thick clouds and thin clouds. Among them, the thick cloud removal algorithm can be further divided into three categories (Lin et al., 2012). The first is based on image restoration methods; The second is based on multi-spectral methods; The third is based on multi-temporal methods. The removal of thin clouds is mainly divided into two parts (G. X. Zhu, 2017). First of all, the cloud area in the remote sensing image is detected, then the cloud coverage area is processed according to the corresponding theoretical algorithm, and the ground feature information is enhanced according to the need, to get the de-cloud image.

Tang et al. (2011) and Liang et al. (2012) all proposed their own thick cloud removal algorithms based on Support Vector Machine (SVM). S. Y. Zhang and Li (2019) proposed a thick cloud restoration algorithm for aerial images based on an improved Criminisi algorithm. Zhao et al. (2016) proposed a thick cloud removal method based on similar pixel replacement, which uses the information of cloud-free areas to reconstruct pixels in cloud and cloud shadow coverage areas. However, if the cloud coverage area is large, this method can not effectively reconstruct the feature information. In the thin cloud removal methods, the filtering method is commonly used, such as the remote sensing image de-cloud algorithm based on improved homomorphic filtering proposed by Zhou et al. (2015), and the thin cloud filtering enhancement method proposed by P. Q. Zhang et al. (2008) .

There are cloud removal algorithms based on multi-spectrum. For example, Xu et al. (2014) use the visible light band of Landsat 8 image and the near-infrared band to remove the cloud. There are also methods for information reconstruction of large areas covered by thick clouds, such as the research on cloud classification algorithm of multi-temporal high-resolution remote sensing images proposed by Salberg (2010). Generally speaking, the method of thin cloud removal is to identify the cloud area at first, and then deal with the cloud coverage area according to the method based on image conversion and enhancement feature information (B. C. Gao et al., 1993, 1998; B. Gao et al., 2002).

Among them, the most classic cloud removal algorithms is the HOT cloud removal method proposed by Y. Zhang et al. (2002).

With the development of remote sensing technology, it is possible to obtain multi-temporal remote sensing images of the same area. In this paper, a multi-temporal remote sensing image fusion de-cloud strategy based on improved BP neural network preprocessing is proposed, which can more effectively restore the ground feature information covered by large thick clouds.

2 Related Work

2.1 Hot Cloud Detection algorithm

Y. Zhang et al. (2002) proposed a HOT cloud removal algorithm in 2002, which uses the correlation between bands in Landsat data to realize cloud detection in multispectral remote sensing images. R. Wang et al. (2015) proposed to use "bright object line" as the basis to replace "clear sky line" to calculate HOT in 2015, to avoid the interference caused by the bright objects in the surface information to the cloud detection.

The advantage of this algorithm is that the requirement of input data is relatively low, and the cloud region can be detected by only one remote sensing image containing red and blue bands, which can easily meet the requirements of most remote sensing data. The disadvantage is that cloud shadow areas cannot be detected automatically.

2.2 Fmask 4.0 Cloud and Cloud Shadow Detection

Fmask (Z. Zhu & Woodcock, 2012; Q. Wang et al., 2018) is a threshold-based cloud detection method by using multi-band information of Landsat 4-8 or Sentinel-2, which can effectively detect and distinguish land, water, snow, ice, cloud, and cloud shadow, and generate masks. Compared with the HOT cloud detection algorithm, it is a more systematic and accurate cloud and cloud shadow detection algorithm.

2.3 Image Fusion for Remote Sensing Images

Image fusion is a process of combining useful information in two or more images to obtain a more comprehensive, accurate, and reliable image description of the same scene. Generally, image fusion can be systematically divided into three levels from low to high: pixel-level fusion, feature-level fusion, and decision level fusion. Pixel-level fusion is the simplest fusion method, and it can retain as much original data as possible. In the application and research, pixel layer fusion methods are common, such as pixel substitution method, linear weighting method, HIS transformation method, PCA transformation method, high-pass filtering method, wavelet transform fusion method, and so on.

2.4 Cloud Removal based on BP Neural Network

R. Wang et al. (2015) proposed a Landsat image cloud removal method based on BP neural network, in which two multi-temporal images (one without cloud and the other with cloud) are used to train the grayscale of some pixels between the images, and the grayscale of the image without cloud is converted to the grayscale similar to that of the image with the cloud.

3 Improved Cloud Removal based on BP Neural Network

3.1 Principle

Since clouds often migrate with the change of time in multi-temporal remote sensing images, we can easily obtain multi-temporal remote sensing images of the same region with different cloud distributions. In this paper, the main principle of the proposed method is as follows. The images with the cloud are used as the input image, and the remote sensing image of another time phase in the same area without overlapping cloud area is used as the auxiliary data (the reference image). Through the image fusion method of pixel replacement, the cloud and cloud shadow covered area in the input image are added from the reference image through pixel replacement, to obtain the cloud-free image after fusion.

The grayscale relationship between multi-temporal images is not completely consistent. Therefore, this cloud removal method requires a BP neural network that uses the gray value group of the common region (non-cloud region) between multi-temporal images as the training data. By the BP neural network preprocessing, the time-phased one image can be transformed into a remote sensing image with a similar gray structure as the time-phase two. After preprocessing, image fusion between multi-temporal remote sensing images is carried out.

This method we proposed is mainly modified for two points in the previous method to reduce human participation. Firstly, the acquisition of remote sensing image cloud and cloud shadow mask is modified. The HOT cloud detection method is replaced by Fmask 4.0 automatic cloud detection algorithm which is widely used and has higher identification accuracy. Secondly, the selection value of BP neural network training is modified. The original grayscale value group marked by classification (Vegetation, waterbody, bare land, residential land, and fields, etc.) is changed to the grayscale value group of the two image's common areas without cloud.

3.2 Method

As shown in Figure 1, after the input image and reference image are obtained, the main steps of this cloud removal experiment are as follows:

1. Data preprocessing.
2. The Fmask 4.0 algorithm is used to detect the cloud and cloud shadow mask of the input images, and then the mask images are extracted and binarized.
3. The cloud and cloud shadow mask images are used to calculate the common cloud-free region of the two images, and the gray value of the common cloud-free region of one scene image is counted as the input value of BP neural network training, and the gray value of the common cloud-free region of the other scene image is taken as the expected output value of the neural network to obtain the mapping relationship.
4. The trained neural network will be used to transform the cloudless image into a spectral structure similar to that of the cloud image.
5. Cloud-free image and mask image after spectral matching are used for image fusion to obtain the resulting image of cloud removal.

4 Experiments and Results

4.1 Process

The experimental data in this study are multi-source remote sensing images of two Landsat landscapes (two sets of experiments with the same satellite source at different

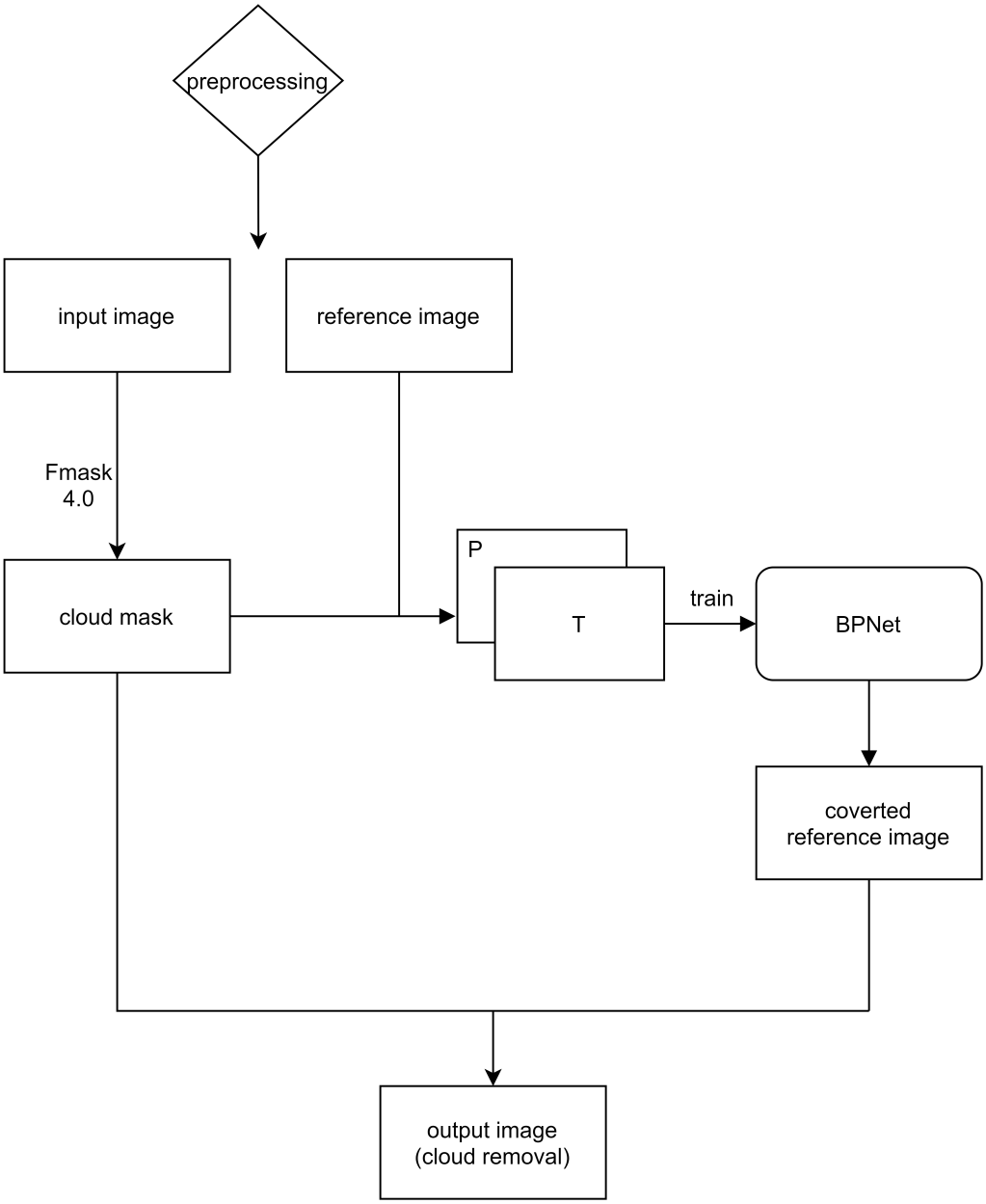

Figure 1. Flow chart of improved cloud removal method based on BPNet.

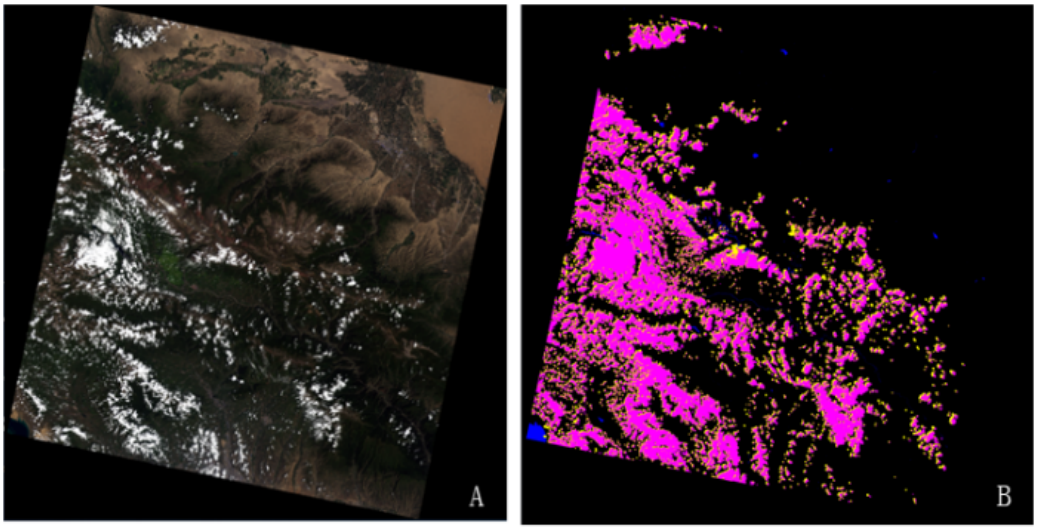

Figure 2. Fmask 4.0 automatic cloud detection result: A. Input image; B. Fmask 4.0 cloud detection result image.

periods and different satellites as remote sensing data sources at different periods), one landscape with cloud, and the other without cloud. A cloudless image was selected for the convenience of fusion as a reference image for comparison, reflecting the effect of cloud removal. However, in practical application, as long as the cloud areas of the two images do not overlap, the effect of cloud removal can be realized.

The pretreatment steps of experimental data are as follows:

1. Download Landsat remote sensing image sets of a different time in the same area, then select one scene with less cloud as the reference image source, and the other scene as the input image source of the cloud to be removed.
2. Open the two scene images respectively, select the center point and image size of the input image and the reference image, so that the area of one scene image is cloudless, and the area of the other scene image is cloudy.
3. By using the coordinates of the center point and the size of the image, the selected area of the two images is intercepted, and the input and reference images of the experiment are obtained.
4. The cloud mask image containing a scene of clouds (as shown in Figure 2) is obtained through the Fmask cloud detection algorithm and binarization was carried out.

Compared with the experimental process before improvement, the cloud removal process in this paper is more convenient, automated, and efficient, which only needs the input image and does not need to do another manual marking. At the same time, the efficiency of obtaining cloud and cloud shadow masks and preparing training values of BP neural network is also faster. Its main manifestations are as follows:

1. In the previous method, manual marking of the cloud center and corresponding cloud shadow center should be carried out on the cloud-containing image before obtaining cloud shadow. Then, several obvious cloud and cloud shadow center points are found to make statistics and obtain the offset vector from cloud to cloud shadow, to calculate the cloud shadow mask map from the cloud mask map and the vec-

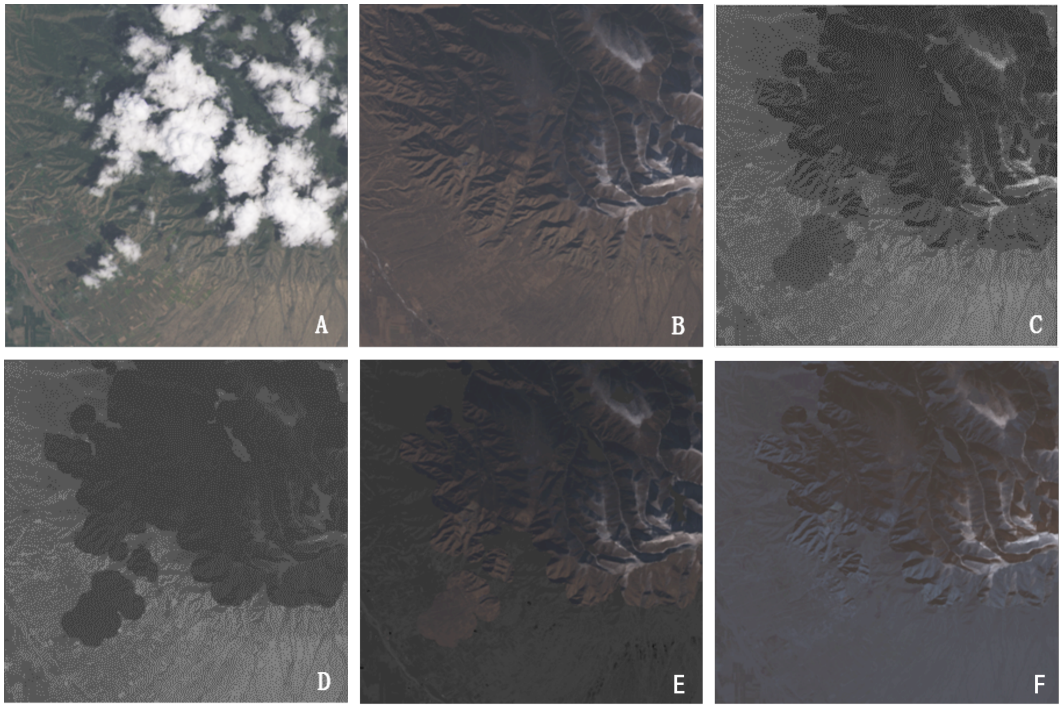

Figure 3. Schematic diagram of input and output images of Experiment 1: A. Input image; B. Reference image; C. Cloud removal image of direct pixel replacement; D. Cloud removal image after linear fitting; E. Cloud removal image after original BPNet processing; F. Cloud removal image after improved BPNet processing.

tor obtained from the statistics. However, in this experimental method, the cloud and cloud shadow automatic detection algorithm of Fmask 4.0 is adopted.

2. In the training preparation stage of the BP neural network, the previous method needs to classify image grayscale categories (such as vegetation, waterbody, bare land, residential land, and field, etc.), and then manually sample several points respectively. With these points as the center, the N*N pixel gray value group of eight connected domains is taken as the input and expected output vector of neural network training. In this paper, on the premise of image registration, according to the obtained cloud and cloud shadow mask image, the grayscale value group of pixels in the two image public areas without cloud is directly adopted as the training value of the BP neural network.

4.2 Results

The data of Experiment 1 are all from Landsat 8, and the longitude and latitude coordinates of the image's center point are (38°2'24.07 "N, 101°5'47.18"). Remote sensing images of 384*384 pixels centering on this center point are intercepted for the cloud removal experiment.

The input and output images of Experiment 1 are shown in Figure 3. Fig. A is an RGB image (natural true color image) synthesized in bands 2, 3, and 4 of cloud remote sensing data, and the data acquisition time is July 22, 2016. Fig. B is the RGB image (reference image) synthesized in bands 2, 3, and 4 without cloud remote sensing data, and the data acquisition time is November 30, 2017.

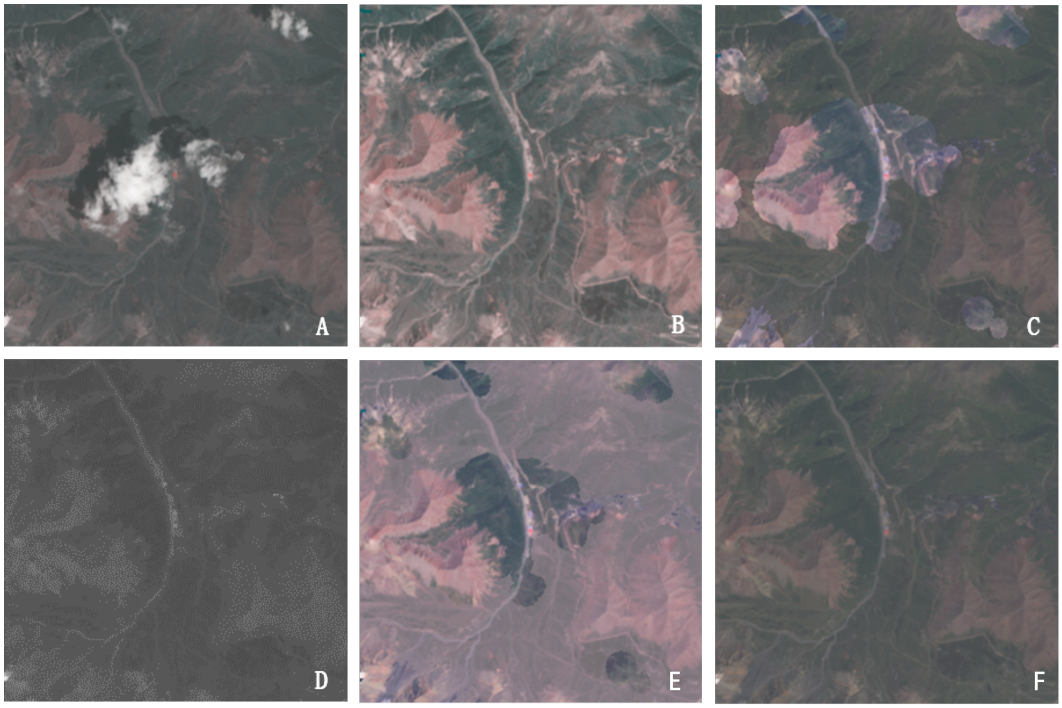

Figure 4. Schematic diagram of input and output images of Experiment 2: A. Input image; B. Reference image; C. Cloud removal image of direct pixel replacement; D. Cloud removal image after linear fitting; E. Cloud removal image after original BPNet processing; F. Cloud removal image after improved BPNet processing.

The data sources of Experiment 2 are Landsat 7 and Landsat 8, which is a multi-source remote sensing data fusion experiment. The central longitude and latitude coordinates of the image are (37°3 '29.99 "N, 101°0' 51.95"), and a remote sensing image of 250*250 pixels centered on this central point is intercepted for cloud removal experiment.

The input and output images of Experiment 2 are shown in Figure 4. Fig. A is the cloud-containing remote sensing data image (input image) of Landsat 8, and the data acquisition time is July 22, 2016. Fig. B is the cloud-free remote sensing data image (reference image) of Landsat 7, and the data acquisition time is July 30, 2016.

4.3 Analysis

4.3.1 Subjective Analysis

Subjectively, it can be observed that the image fusion method of pixel replacement can achieve the effect of removing thick clouds. Compared with direct pixel replacement or pixel replacement after linear fitting pretreatment, our method has a better subjective cloud removal effect. The details are as follows:

1. In Experiment 1, the grayscale transition effect at the junction of cloud and the cloudless image is better, and the "color difference" is smaller.
2. In Experiment 2, the ground object information in the cloud removal effect of the method presented in this paper is more clearly visible, especially the mountainous part in the lower right corner of the image.

Table 1. SSIM and COSINE in Experiment 1.

Item	SSIM	COSINE
Figure A and Figure B	0.6087	0.8731
Figure E and Figure B	0.8770	0.9898
Figure F and Figure B	**0.9387**	**0.9962**

Table 2. SSIM and COSINE in Experiment 2.

Item	SSIM	COSINE
Figure A and Figure B	0.8217	0.9548
Figure E and Figure B	0.9338	0.9944
Figure F and Figure B	**0.9785**	**0.9991**

4.3.2 Objective Analysis

Objectively, SSIM and cosine similarity of the image are used to evaluate the cloud removal effect of Experiment 1 and Experiment 2. The statistical tables are as follows (Table 1 and Table 2).

It can be seen intuitively from Table 1 and Table 2 that the de-cloud method in this paper has a higher similarity with the reference image in terms of image vector correlation and image structure.

5 Conclusions

In this paper, the Fmask algorithm is used to obtain mask images, and an improved cloud removal strategy for remote sensing images based on BP neural network is proposed. Two multitemporal remote sensing images with a similar spectral structure are obtained after preprocessing by BP neural network. Image fusion of multi-source remote sensing images is realized through pixel replacement between multi-temporal remote sensing images to achieve the effect of cloud removal. Compared with the existing methods, the method presented in this paper is simpler and more automatic in the operation process and achieves cloud removal of remote sensing images more efficiently.

Acknowledgments

This work is supported by the Young and Middle-aged Scientific Research Fund Project of Qinghai University under Grant No. 2019-QGY-4 and the Natural Science Foundation of China under Grant No. 61863031.

References

Gao, B., Yang, P., Han, W., Li, R., & Wiscombe, W. (2002). *An algorithm using visible and 1.38-μm channels to retrieve cirrus cloud reflectances from aircraft and satellite data, ieee t. geosci. remote, 40, 1659–1668.*

Gao, B. C., Goetz, A. F., & Wiscombe, W. J. (1993). Cirrus cloud detection from airborne imaging spectrometer data using the 1.38 μm water vapor band. *Geophysical Research Letters*, *20*(4), 301–304.

Gao, B. C., Kaufman, Y. J., Han, W., & Wiscombe, W. J. (1998). Corection of thin cirrus path radiances in the 0.4–1.0 μm spectral region using the sen-

sitive 1.375 μm cirrus detecting channel. *Journal of Geophysical Research: Atmospheres*, *103*(D24), 32169–32176.

Guo, L. M. (2017). Research of cloud and shadow removal alogorithm for landsat satellite image. *Guangxi Normal University*, 1–z.

Liang, D., Kong, J., & Hu, G. S. (2012). Thick cloud and cloud shadow removal of remote sensing image based on support vector machine. *Acta Geodaetica et Cartographica Sinica*, *41*(2), 225–231.

Lin, C. H., Lai, K. H., & B., Z. (2013). Patch-based information reconstruction of cloud-contaminated multitemporal images. *IEEE Transactions on Geoscience and Remote Sensing*, *52*(1), 163–174.

Lin, C. H., Tsai, P. H., & Lai, K. H. (2012). Cloud removal from multitemporal satellite images using information cloning. *IEEE transactions on geoscience and remote sensing*, *51*(1), 232–241.

Salberg, A. B. (2010). Land cover classification of cloud-contaminated multitemporal high-resolution images. *IEEE Transactions on Geoscience and Remote Sensing*, *49*(1), 377–387.

Shi, Q. (2018). *Accurate cloud and cloud shadow detection in multispectral remote sensing images* (Unpublished doctoral dissertation). University of Electronic Science and Technology of China.

Tang, W. Q., Liang, D., & Hu, G. S. (2011). Thick cloud removal algorithm of remote sensing image based on support vector machine. *Remote Sensing Technology and Application*, *26*(1), 111–116.

Wang, Q., Huang, C., & Liu, G. H. (2018). Cloud shadow identification based on qa band of landsat 8. *Journal of Geo-information Science*, *1*, 89–98.

Wang, R., Wei, C. T., Ma, Y. D., & Hu, T. (2015). Bp ann algorithm for removing cloud in landsat data. *Journal of Guilin University of Technology*, *35*(3), 535–539.

Wei, Y. C., Tang, G. A., & Yang, X. (2015). *Course of remote sensing digital image processing*. Ke xue chu ban she.

Xu, M., Jia, X. P., & Pickering, M. (2014). Automatic cloud removal for landsat 8 oli images using cirrus band. In *2014 ieee geoscience and remote sensing symposium* (pp. 2511–2514).

Zhang, P. Q., Yu, X. C., & Han, L. (2008). Remote sensing image enhancement using filtering methods with thin cloud cover. *Hydrographic Surveying and Charting*, *28*(2), 13–16.

Zhang, S. Y., & Li, C. L. (2019). Thick cloud restoration of aerial images based on improved criminisi algorithm. *Laser & Optoelectronics Progress*, *55*(12), 121012.

Zhang, Y., Guindon, B., & Cihlar, J. (2002). An image transform to characterize and compensate for spatial variations in thin cloud contamination of landsat images. *Remote Sensing of Environment*, *82*(2-3), 173–187.

Zhao, M. Y., Zheng, X. S., & Liu, W. J. (2016). Research on thick cloud removal of remote sensing image based on similar pixel replacement. *Application Research of Computers*, *33*(11), 3509–3512.

Zhou, X. J., Guo, J., & Zhou, C. X. (2015). An algorithm of cloud removal for remote sensing image based on improved homomorphic. *Radio Engineering*, *3*, 14–18.

Zhu, G. X. (2017). *The method of image de-noising by fusing multi-temporal remote sensing images* (Unpublished master's thesis). Shanghai Ocean University.

Zhu, Z., & Woodcock, C. E. (2012). Object-based cloud and cloud shadow detection in landsat imagery. *Remote sensing of environment*, *118*, 83–94.